

AN EMPIRICAL MODEL OF ELECTRON ENERGY TRANSPORT IN THE PRESENCE OF RATIONAL SURFACES IN W7-AS

R. Brakel, M. Anton, J. Geiger, H.-J. Hartfuß, G. Kühner, A. Weller, E. Würsching,
W7-AS Team, ECRH-Group

Max-Planck-Institut für Plasmaphysik, EURATOM Association, Garching, Germany

1. Introduction

At W7-AS, a stellarator with small shear in the vacuum field, systematic studies of ECRH-discharges being dominated by electron heat transport have shown a strong dependence of confinement on both the boundary value $-a$ of the rotational transform and the magnetic shear, the latter being controlled by an inductive current I_{OH} [1, 2]: (i) With small net plasma current, $I_p = I_{BS} + I_{OH}$ (I_{BS} is the bootstrap current), i.e. at low or moderate shear, optimum confinement is found close to the major resonances $-a = 1/2, 1/3$, etc., being a factor of about 2 higher than at other $-a$ -values. (ii) With high net currents, i.e. at high shear, confinement improves to the optimum level for any $-a$. Similar behaviour was already observed in W7-A, with the difference that the $-a$ -dependence of confinement vanishes with increasing shear but at a level lower than the optimum. This was interpreted by the overlap of magnetic islands, the latter arising from external perturbation fields, when shear becomes too large [3]. (It should be noted that the maximum average current density $I_p/(a^2)$ was smaller by a factor of about 2.5 in the W7-A experiments).

For several reasons, the dependencies found in W7-AS can hardly be explained by island formation at $-a$ -values being in resonance with the major Fourier components of the external perturbation spectrum, i.e. the „natural“ $5/m$ components from the fivefold toroidal periodicity and $1/2, 1/3$, etc., components from field errors: (i) Confinement degradation is also observed for $-a$ -values, e.g. 0.48, where nested closed flux surfaces without islands exist in the vacuum field [4]. (ii) The perturbation amplitudes rapidly decrease towards the magnetic axis. In the experiment, however, the plasma radius was reduced by the movable top/bottom limiters. (iii) Large shear would lead to island overlap and ergodization, which is in contradiction to the observed improvement of confinement. (iv) A confinement model [4] which short-circuits the electron transport over island regions, their width and location being determined from the perturbation field spectrum by a field mapping procedure [3], does not reproduce the experimental dependencies. However, the model does not self consistently account for the coupling of transport and $-a$ -profile.

The $-a$ -ranges of optimum confinement near low order rationals are characterized by the absence of higher order rational values [3]. For the other ranges, where confinement is degraded, it is therefore assumed that internal perturbations arising at such higher order rational surfaces, e.g., from turbulence or MHD activity enhance the electron energy transport [5]. This aspect could also be considered in the interpretation of the recently reported internal electron transport barriers at low order rationals in the RTP-tokamak [6].

This paper reviews in chapter 2 a simple model [5], which selfconsistently couples electron heat transport and rotational transform profile by a parametric ansatz for the electron heat conductivity, χ_e , which depends on the occurrence of rational q -values and magnetic shear in their vicinity. The ansatz is based on the analysis of stationary plasmas with inductive net current control by the Ohmic transformer, heated by 450 kW ECRH with the density, $n_e = 4 \times 10^{19} \text{ m}^{-3}$, kept constant by feedback controlled gas puffing ($B = 2.5 \text{ T}$, $R = 2 \text{ m}$, $a = 0.15 \text{ m}$, $\beta_0 = 0.6\%$, $T_i = 450 \text{ eV}$, for experimental details see [1, 2]). At the present stage of the model, particle transport is not considered. As a first approximation this seems to be justified for this type of discharges, since the experimental density profiles are rather robust against changes in the magnetic configuration. The dependencies observed in confinement are mainly due to changes of the electron temperature gradient in the outer half of the confinement volume. In chapter 3, the model is used to predict confinement in discharges without external loop voltage where the plasma current is determined by the bootstrap current ($I_p = I_{BS}$, $I_{OH} = 0$). The results compare well experimental data.

2. The model

The basic observations, i.e. that confinement is at the optimum in the absence of rational q -values, degrades when shear is low in the presence of rationals, and re improves when shear is increased, are comprised in a simple ansatz for the electron heat conductivity, χ_e :

$$\chi_e(r, q) = \chi_{neo}(r) + \chi_0(r) + \sum_{nm} \chi_{nm}(r, q),$$

$$\chi_0 = \exp(-c_i (r/a)^i) \text{ m}^2/\text{s}, \quad \chi_{nm} = \chi_{nm} \exp(-|q - n/m| - |r - r_{nm}|)$$

For the neoclassical heat conductivity, χ_{neo} , being significant only in the center for most conditions considered, an axisymmetric approximation is used [7]. χ_0 accounts for the anomalous transport at optimum confinement which still exists in particular in the boundary region. The functional r -dependence of χ_0 has been chosen arbitrarily, the parameters c_i being adjusted to reproduce the experimental electron temperature profile, $T_e(r)$, in the absence of resonances. The basic point of the model is, that close to a rational surface, $q = n/m$, χ_e is additionally increased by χ_{nm} . These enhancements χ_{nm} are exponentially damped with increasing absolute value of shear, $q = d/d-r$, and with the distance between the radial position r and the radius r_{nm} of the rational surface, as is seen by the Taylor expansion $(q - n/m) \approx (r - r_{nm}) / (R - r_{nm})$. The constants χ_{nm} , c_i , and i and the maximum m -number, m_{max} , to be considered in the sum over rationals have to be determined by comparison with experimental data.

The rotational transform profile is determined by the pressure driven bootstrap current density, j_{BS} , and – if an inductive current contributes – the inductive current density, j_{OH} :

$$-q(r) = -q_{ex}(r) + \mu_0 R / (B r^2) \int_0^r (j_{BS} + j_{OH}) r dr$$

$-q_{ex}$ is the nearly shearless external rotational transform. Pfirsch-Schlüter currents are neglected due to moderate β . Since the bootstrap current in W7-AS is tokamak-like [8], the

approximation $j_{BS} = f_{BS} j_{BS}^{HH}$ is used, with j_{BS}^{HH} being the bootstrap current density in a circular tokamak [7]. The factor f_{BS} accounts for the mean elongation of the W7-AS flux surfaces. Its value has been determined to be in the range 0.5 to 0.7 by comparison with DKES calculations and current balance analysis. For simulating discharges with inductive net current control, j_{OH} is calculated from the tokamak neoclassical conductivity [7] and normalized such that bootstrap and inductive current add up to the given net plasma current I_p .

Given the current densities, and thus $-j(r)$, $n_e(r)$ can be calculated to be used in the purely diffusive power balance

$$dT_e / dr = -(4 \pi R r n_e)^{-1} P_{heat}$$

to obtain the electron temperature profile. $n_e(r)$ and $P_{heat}(r)$ are density and power deposition profiles, respectively. Since the heat conductivity, being a function of T_e , implicitly depends on the temperature profile via the current densities, the set of equations is selfconsistently solved by an iteration procedure which starts with an initial profile for $T_e(r)$. For some conditions, e.g. when magnetic shear is low and $-j(r)$ is close to the transition from a resonance free region to a region with densely spaced resonances, convergence of the iteration is poor. Convergence is obtained by a damping algorithm, which uses the weighted average $(y_i + w y_{i-1}) / (1+w)$, with $w = 4$, of the last two iteration steps as input for the next iteration, where y may be n_e or j_{BS} .

Density profile (adapted from experiment) and power deposition profile (Gaussian shaped power density with 2 cm HWHM), the external rotational transform and, optionally, a net plasma current are input to the calculation. For all conditions, $f_{BS} = 0.7$, $Z_{eff} = 2$ (required for the neoclassical calculations) and the boundary condition $T_e(a) = 100$ eV are used. Good agreement between experimental data and model calculations have been obtained, for both the electron temperature profile and global confinement, with the following set of model parameters [5]: $m_{max} = 20$, $\nu = 0.004$, $a = 1.1$ m, $\nu_{nm} = 1.1 g_{nm}^{-1} m^2/s$ for n/m (g_{nm} is the degeneracy of a n/m -value, i.e. every rational number is counted only once) and $c_0 = -0.23$, $c_2 = -2.3$, $c_6 = 4.6$, other $c_i = 0$ for $i \neq 0, 2, 6$ (NOTE: by a mistake the values of c_i given in Ref. [5] are those for the polynomial representation of $\log(\nu)$ instead of $\ln(\nu)$).

3. Bootstrap current dominated discharges

When the boundary value of the total rotational transform, $-j_a = -j_{ex,a} + -j_r$, where $-j_r$ is the plasma current contribution, is fixed by inductive current control the iteration procedure converges to a unique solution for any $-j_{ex,a}$, independent of the initial conditions. When the constraint of a fixed net plasma current is relaxed, the current ($I_p = I_{BS}$) selfconsistently couples to confinement and a bifurcation like phenomenon occurs. Fig. 1 shows for the volume integrated electron kinetic energy and for the bootstrap current that two branches of confinement exist in windows of $-j_{ex,a}$ below the regions of optimum confinement, i.e. $-j_{ex,a} < 1/2$ and $< 1/3$, where confinement is usually low. The high and low confinement branches are obtained by starting the iteration with a high ($T_{e,0}(r=0) = 2.5$ keV) or low ($T_{e,0}(r=0) = 0.75$ keV) T_e -profile, respectively. The profile form is the experimental one for high confinement in Fig. 3 (for n_e the absolute profile of Fig. 3 has been used). The curves in Fig. 1 are labeled

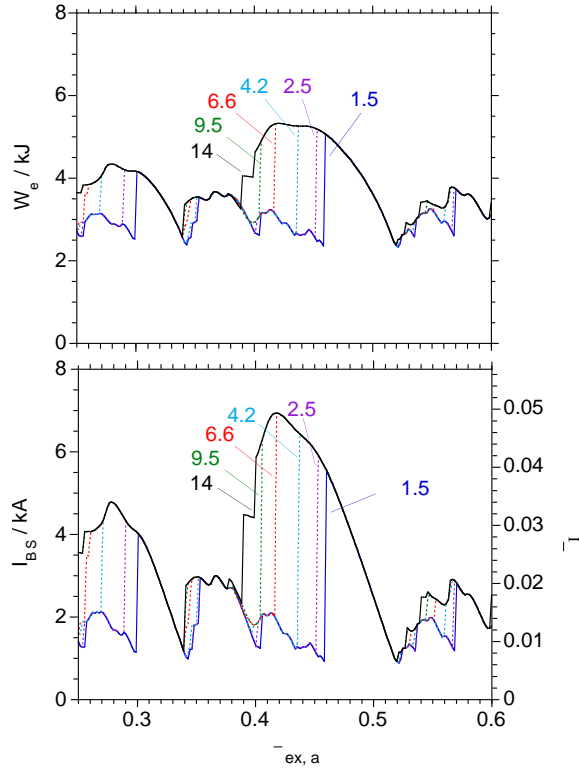


Fig. 1: Calculated dependence of electron kinetic energy and bootstrap current on $-_{ex,a}$ showing two branches of confinement. The curves are labeled by the bootstrap current corresponding to the initial T_e -profile for the iteration. ($B = 2.5$ T, $P = 400$ kW, $n_e = 4 \times 10^{19} \text{ m}^{-3}$, $I_{OH} = 0$, $r_{dep} = 0$ cm)

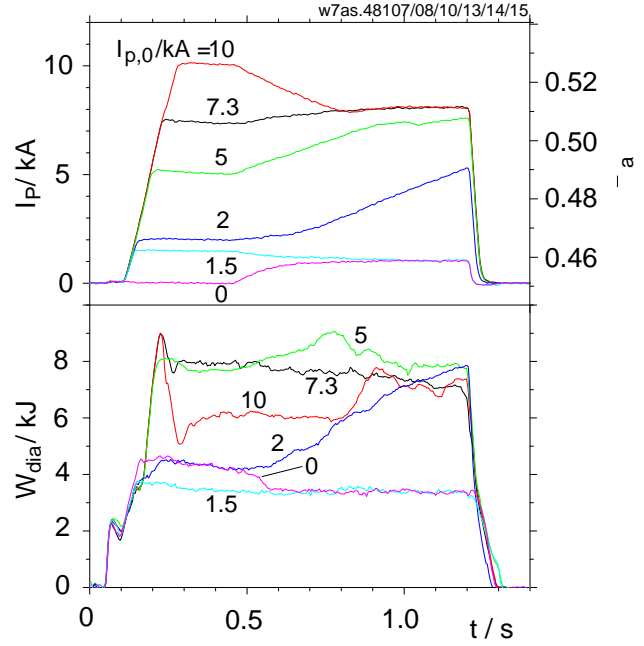


Fig. 2: Evolution of plasma current and diamagnetic energy for discharges with different initial inductively controlled currents. The external loop voltage is switched off at 0.45 s. ($B = 2.5$ T, $P = 400$ kW, $n_e = 4 \times 10^{19} \text{ m}^{-3}$, $-_{ex,a} = 0.45$)

by the bootstrap current $I_{BS,0}$ which corresponds to the initial T_e -profile, the limiting cases corresponding to $I_{BS,0} = 14$ kA and 1.5 kA, respectively. The $-_{ex,a}$ -window where the high confinement solution is reached narrows when the initial current decreases.

At high confinement a correspondingly high bootstrap current (i) produces magnetic shear thereby reducing transport and – even more important – (ii) shifts the rotational transform from its vacuum field value into the next resonance free region, e.g. around $- = 1/2$ ($-_r$ is indicated on the right hand scale in Fig.1). Optimum confinement is therefore predicted for external $-$ -values well below the next low order rational (e.g. 0.42 in Fig. 1). For the experiment this implies that a critical initial current drive must be provided to reach the high confinement branch. Otherwise the discharge will remain at low confinement, where the bootstrap current is not sufficiently high.

The predicted bifurcation could be demonstrated experimentally in a sequence of discharges at $-_{ex,a} = 0.45$ (Fig. 2). The plasma current is first ramped to various initial values $I_{p,0}$ by the Ohmic transformer. After a flat top phase of some 100 ms, the external loop voltage is switched off at 0.45 s by keeping the transformer current constant until the end of the discharge, allowing the plasma current to evolve freely according to the L/R -time and to the temporal changes in confinement. Two stable regimes can be identified. When the initial current is below 1.5 kA, both plasma current and diamagnetic energy, evolve to identical

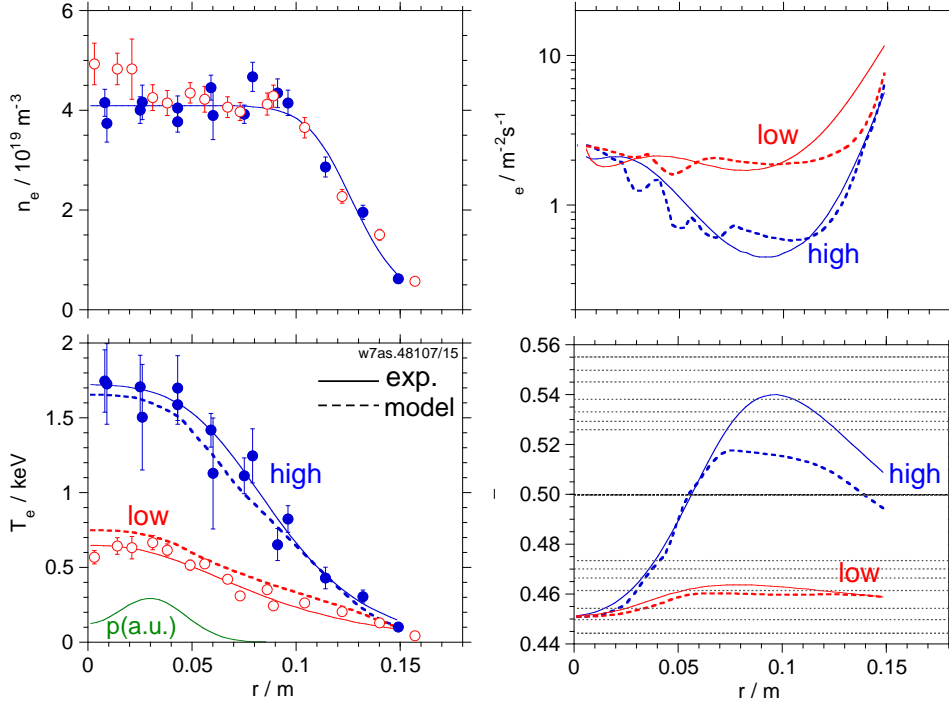


Fig. 3: Radial profiles for low and high confinement. Dashed lines: model. Full lines and data points: experiment (discharges with $I_{p,0} = 0$ and 7.3 kA of Fig. 2 at $t = 1.0$ s, data: Thomson scattering, e_e from power balance, $-$: calculated from bootstrap current normalized to plasma current). The assumed power density profile is indicated. Horizontal lines: rational $-$ values up to $m = 20$

stationary values at low levels of 1.0 kA and 3.3 kJ, respectively. All discharges with $I_{p,0} = 7.3$ kA converge to nearly steady state conditions with high confinement at $I_p = 8.0$ kA and $W_{dia} = 7.5$ kJ. At intermediate values, 2 kA $I_{p,0} < 5$ kA, I_p and W_{dia} steadily increase not becoming stationary within the discharge time. Thus, for the particular value $-_{ex,a} = 0.45$ the discharge bifurcates at a critical initial current between 1.5 and 2.0 kA.

Disregarding the difference between $I_{BS,0}$ and $I_{p,0}$, the initial current for bifurcation is in rough agreement with the prediction of Fig. 1, where for $I_{BS,0} = 2.5$ kA the transition occurs at $-_{ex,a} = 0.45$ (the damped iteration in the calculation can formally be interpreted as an evolution in time). This formal coincidence must not be over-emphasized. For Fig. 1, a central ECRH-deposition was used, whereas the experimental T_e -profiles indicate off-axis deposition at $r_{dep} = 3$ cm. With off-axis deposition, experimental and simulated steady state plasma profiles for low and high confinement are in rather good agreement (Fig. 3). However, the predicted transition at $-_{ex,a} = 0.45$ occurs now for $I_{BS,0} = 5$ kA. Another uncertainty is due to a possible EC driven current (up to ± 1 kA) which cannot be ruled out for the experiment.

A mode and frequency analysis of the magnetic fluctuations, measured by a poloidal array of 16 Mirnov probes, is shown in Fig. 4. In the final state of low confinement a broad band of activity between 35 and 65 kHz is observed. A low mode number is indicated by the analysis. But this would also be consistent with high mode numbers which cannot be resolved by the array. These fluctuations disappear in the high confinement state. The absolute level of the fluctuations is low even in the first case ($B/B = 3 \times 10^{-5}$), and it can therefore not be concluded that magnetic fluctuations are responsible for enhanced transport.

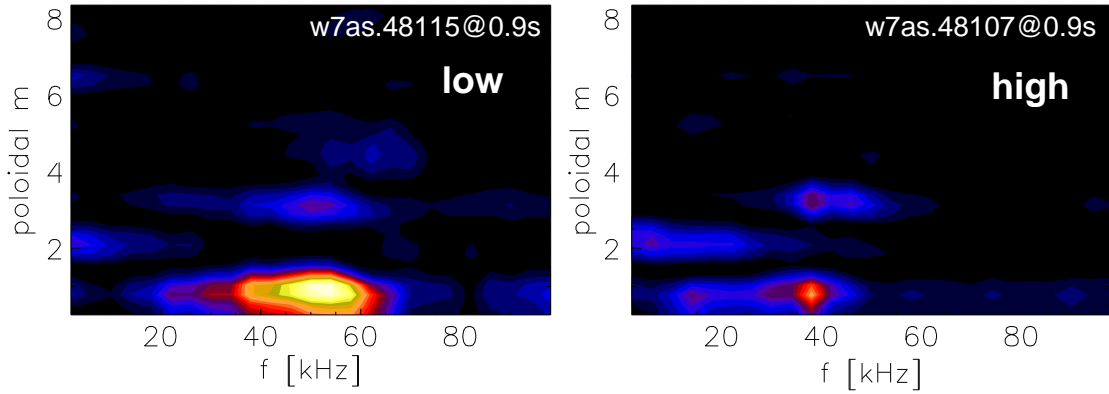


Fig. 4: Contour plot of magnetic fluctuation intensity measured by a poloidal array of 16 Mirnov probes as a function of frequency and poloidal mode number at low (left) and high (right) confinement.

In Fig. 5 a full time evolution from low to high confinement is constructed by shifting the time scale of the discharges at $I_{p,0} = 2, 5,$ and 7.3 kA such that their traces continuously match. The time for the plasma current to reach steady state is 2.5 s. In the first phase of improvement (0.5 to 0.8 s) the gradient of the T_e -profile strongly steepens, then the profile continuously broadens. Similar features are observed for the density, but being much less pronounced. After a transient optimum at 1.5 s confinement tends to become stationary, but stationarity is not really reached. Starting from the center the temperature slowly decreases in time for $t > 1.9$ s at still rising current. This is preceded by the onset of a bursting central mode activity at $t = 1.7$ s, as can be seen on the central temperature channel. The activity is located within $r < 5$ cm and causes temperature variations of up to 250 eV within this radial range. An even m -number is deduced from soft-x and ECE-data, and it is probably related to

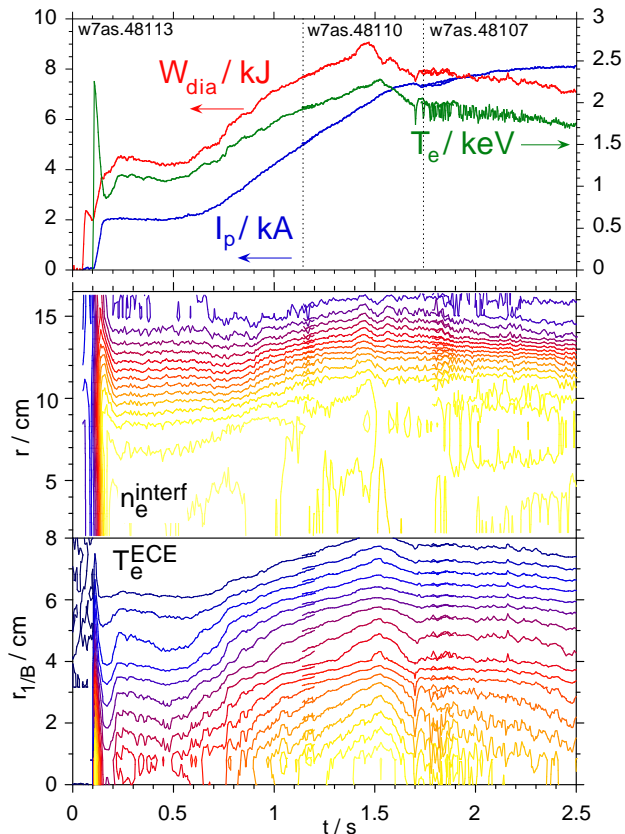


Fig. 5: Evolution to steady state plasma current at high confinement of W_{dia} , I_p and central T_e (from ECE) and of the radial profiles of T_e and n_e (contour lines from interferometry and ECE, $r_{1/B}$ is approximately $0.5 r$). The extended timescale is obtained by shifting the traces of the $2, 5$ and 7.3 kA discharges in Fig. 2 such that they continuously match.

the existence of $- = 1/2$ at $r = 5$ cm (Fig. 3). A $-$ -code analysis predicts tearing mode instability, which would then be driven by the bootstrap current.

4. Discussion

As reported earlier [5], confinement in ECR-heated discharges in W7-AS can be well described by a simple model which assumes enhanced electron energy transport in the presence of rational surfaces and a reduction of enhanced transport with increasing shear. The model, originally derived from experiments with inductive net current control, has now been applied to scenarios without external loop voltage („true“ stellarator operation). This introduces an additional degree of freedom, leading to a bifurcation phenomenon with states of low and high confinement for identical external control parameters. Depending on the initial conditions the close coupling of transport, bootstrap current and rotational transform may shift the total $-$ from unfavourable vacuum field values with densely spaced rational surfaces upwards into the next resonance free region or not. The basic features of this prediction could be demonstrated experimentally, with an inductively driven current being applied in the start-up phase as the bifurcation parameter. At a critical initial current the discharge bifurcates to low or high confinement when the external loop voltage is switched off.

In the high confinement state magnetic fluctuations in the boundary region nearly disappear. However, the discharge slowly deteriorates from the center, probably due to a bootstrap current driven $m = 2$ tearing mode. The occurrence of $- = 1/2$ close to the center should move to smaller radii by more central heating. It can possibly be completely avoided by a reduction of $-_{ex,a}$ and a central EC driven co-current. The latter would compensate the $-_{ex,a}$ -reduction at the boundary and simultaneously raise the central $-$.

The agreement between model and experimental findings supports the hypothesis of enhanced electron energy transport in the presence of rational surfaces. Moreover, the results elucidate once more that, in order attain experimental control of optimum confinement in stellarators with low vacuum field shear, it is very important to keep the confinement dependend excursions of the boundary value of the rotational transform small. In the standard operation mode of W7-AS this is achieved by inductive net current control, in the optimized W7-X by a strong reduction of both the bootstrap and Pfirsch-Schlüter current [9].

References

- [1] R. Brakel et al., *Plasma Phys. Control. Fusion* **39B**, 273 (1997)
- [2] R. Brakel et al., *J. Plasma and Fusion Res. SERIES* **1**, 80 (1998)
- [3] H. Wobig et al., *Plasma Phys. and Control. Nucl. Fusion Res.* (Proc. 11th Int. Conf. Kyoto, 1986) Vol. 2 (IAEA: Vienna) 369 (1987)
- [4] R. Jänicke, *Nucl. Fusion* **33**, 687 (1993)
- [5] R. Brakel et al., Proc. 25th EPS Conf. Contr. Fusion and Plasma Phys., Prague, p. 423 (1998)
- [6] N. Lopes-Cardozo, *Plasma Phys. and Control. Nucl. Fusion Res.* (Proc. 17th Int. Conf. Yokohama, 1998) IAEA-F1-CN-69/EX7/4
- [7] F. L. Hinton and R. D. Hazeltine, *Rev. Mod. Phys.* **48**, 239 (1976)
- [8] C. Wendland et al., Proc. 26th EPS Conf. Contr. Fusion and Plasma Phys., Maastricht, p. 1489 (1999)
- [9] G. Grieger et al., *Phys. Fluids B* **4**, 2081 (1992)